



Temperature and Concentration Effects on Oscillatory Flow for Variable Viscosity Carreau Fluid through an Inclined Porous Channel

Dheia G. Salih Al-Khafajy, Jubran Abdulameer Labban*

Department of Mathematics, College of Science, University of Al-Qadisiyah, Diwaniya, Iraq

Abstract

The aim of this paper is to study the combined effects of the concentration and the thermo-diffusion on the unsteady oscillation flow of an incompressible Carreau fluid through an inclined porous channel. The temperature is assumed to affect exponentially the fluid's viscosity. We studied fluid flow in an inclined channel under the non-slip condition at the wall. We used the perturbation series method to solve the nonlinear partial differential equations. Numerical results were obtained for velocity distribution, and through the graphs, it was found that the velocity of fluid has a direct relation with Soret number, Peclet number, and Grashof number, while it has a reverse variation with chemical reaction, Schmidt number, frequency of oscillation, and Froude number.

Keywords: Oscillatory flow, Carreau fluid, Inclined porous medium, Perturbations method.

تأثير درجة الحرارة والتركيز على التدفق التذبذبي لمائع كاريو ذو اللزوجة المتغيرة خلال قناة مسامية مائلة

ضياء غازي صالح الخفاجي, جبران عبد الامير خطار اللبان*

قسم الرياضيات كلية العلوم, جامعة القادسية, الديوانية, العراق

الخلاصة

هدف هذا البحث هو دراسة التأثيرات المشتركة للتركيز والانتشار الحراري على التدفق التذبذبي لمائع كاريو الغير قابل للانضغاط خلال قناة مسامية مائلة. من المفترض أن تؤثر درجة الحرارة بشكل كبير على لزوجة المائع. درسنا تدفق المائع في قناة مائلة تحت شرط عدم الانزلاق عند الجدار. استخدمنا طريقة سلسلة الاضطراب لحل المعادلات التفاضلية الجزئية غير الخطية. تم الحصول على نتائج عددية لتوزيع السرعة، ومن خلال الرسوم البيانية، وجد أن سرعة المائع تتناسب طردياً مع عدد سورت، عدد بيكلت وعدد غراشوف، بينما تتناسب سرعة المائع عكسياً مع التفاعل الكيميائي، عدد شميدت، عدد فرويد وتردد التذبذب.

Introduction

The oscillatory flow is very important to study blood dynamics in the arteries and veins to prevent cardiovascular diseases, as a flow of Carreau fluid in a diagonal channel indicates the nature of blood flow in the human body. Mathematical modelling of blood dynamics helps to understand this phenomenon *in vivo*. Theoretical and practical investigations can reveal important relationships between the oscillatory flow of the Carreau fluid in the closed duct and the movement of blood in the arteries and other blood vessels. Many researchers presented their scientific results related to

*Email: Jubran.Labban@qu.edu.iq

oscillatory flow of different flow engineering (Poiseuille and Couette flows) and they were among the first researchers in this field [1, 2]. Recently, many researchers investigated the oscillatory flow [3- 6].

The viscosity of fluids is of great importance in the fields of industrial food, medicine, and other sciences. There are many studies in the scientific literature on the movement of viscous fluids in the canal. Person [7] discussed the effect of high temperature on the flow of viscous fluids through channels. Al-Khafajy [8] developed a model that treats the oscillating flow of a viscous Jeffrey fluid through a porous channel and found that the velocity of a variable viscosity fluid is lower than that of a fluid with a fixed viscosity, under the same conditions for both cases. Peristalsis of Sisko fluids with variable viscosities was investigated by Tanveer *et al.* [9]. The influence of heat transfer on MHD oscillatory flow for Williamson fluid with variable viscosity through a porous medium was investigated by Khudair and Al-khafajy [4]. Increased interest has led to study the effects of temperature with the focus on fluid movement in recent years. Most research confirmed that the increase in temperature increases the velocity of the fluid, while the fluid velocity changes in an unclear manner with the difference in concentration and according to the location of the fluid in the canal [10- 13]. In nature, most of the flow channels, especially in the human body, are inclined channels. For this reason, there was a great interest in the recent period on fluid flow through inclined channels, as many researchers presented mathematical models in different fluid flow values in inclined channels [13- 15].

The present analysis aims to discuss the combined effects of the concentration and the thermo-diffusion on the unsteady oscillatory flow for Carreau fluid with variable viscosity through an inclined porous channel. Such attempt has not yet been explored, to the best of our knowledge. This paper consists of five sections, the first of which is the current one "Introduction". The second section includes formulating the governing equations with the boundary conditions, in addition to the basic equation for Carreau fluid with variable viscosity. The third section includes solving the problem. We discuss the effects of parameters affecting the velocity of the fluid through graphs in the fourth section. The last section briefly reviews the most important parameters on the problem.

MATHEMATICAL FORMULATION

Consider the unsteady oscillation flow of an incompressible Carreau fluid with variable viscosity between two parallel porous plates which are inclined in an upward extending in the x -axial direction. The width ($2l$) is much smaller than the length of the channel so that the flow is approximately in one direction. As shown in Figure-1, the Cartesian coordinate system may be chosen for the channel, whereas x is taken as the coordinate axis parallel, whereas y is perpendicular, to the channel plates. Also, we set the no-slip boundary conditions for the movement of fluid through the channel while the two walls of the channel are held at different temperatures T_{-l} and T_l (with $T_{-l} < T_l$) and different concentrations C_{-l} and C_l (with $C_{-l} < C_l$), respectively. Moreover, there is an inclined channel making an angle σ with the horizontal (x -axis) and an angle φ with the vertical (y -axis).

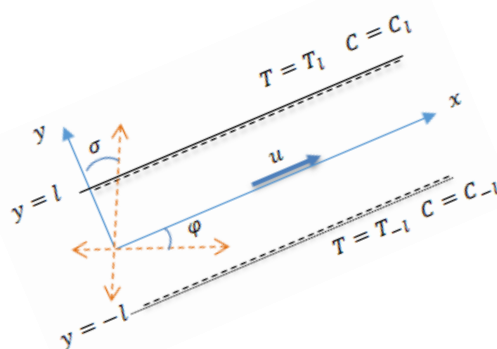


Figure 1- Design of the problem(inclined flow channel)

The governing equations of the problem are given by:

$$\text{The continuity equation: } \nabla \cdot V = 0 \quad (1)$$

The momentum equations: $\rho \frac{DV}{D\bar{t}} = \nabla \cdot \mathbf{S} + \beta_1 \Delta T + \beta_2 \Delta C - \frac{\mu(T)}{k} V + \rho g(\text{isin}\varphi - \text{jcos}\varphi)$ (2)

The concentration equation: $\frac{DC}{D\bar{t}} = \nabla \cdot \left(D_c \nabla C + \frac{D_c T_d}{T_m} \nabla T \right) - K_r^* \Delta C$ (3)

The temperature equation: $\rho c_p \frac{DT}{D\bar{t}} = \nabla \cdot (T_c \nabla T) - \nabla \cdot Q_r + h_g \Delta T$ (4)

where $V = (u(y, t), 0, 0)$ is velocity field, $T = T(y, t)$ is temperature, $C = C(y, t)$ is concentration, $\frac{\partial Q_r}{\partial y} = 4\alpha^2(T_{-l} - T)$ is a radiation heat flux, α is a radiation absorption, $\beta_1 = \rho g \beta_T \sin(\sigma)$, $\beta_2 = \rho g \beta_C \sin(\sigma)$, ρ is a density, \mathbf{g} is a gravity field, c_p is a specific heat at constant pressure, T_c is a thermal conductivity, h_g is a heat generation, D_c is a coefficient of mass diffusivity and T_d is a thermal diffusion ratio. The velocity, concentration, and temperature at the inclined walls of the channel are given as:

$\bar{u} = 0$ at $\bar{y} = \pm l$. (5)

$C = C_{-l}$, $T = T_{-l}$ at $\bar{y} = -l$ and $C = C_l$, $T = T_l$ at $\bar{y} = l$. (6)

The basic equation for Carreau fluid with variable viscosity is given as:

$\mathbf{S} = -\bar{p}\mathbf{I} + \bar{\tau}$

$\bar{\tau} = \left[\mu_\infty + (\mu(T) - \mu_\infty) (1 + (Y\dot{\gamma})^2)^{\frac{n-1}{2}} \right] (\nabla \bar{V} + (\nabla \bar{V})^T)$

where $\bar{\tau}$ is extra stress tensor, \bar{p} is pressure, \mathbf{I} is unit tensor, Y is time constant, μ_∞ is infinite shear rate viscosity and $\mu(T)$ is variable viscosity. In the case of $Y < 1$ and $\mu_\infty = 0$, we can write:

$\bar{\tau} = \mu(T) \left[1 + \left(\frac{n-1}{2} \right) Y^2 \dot{\gamma}^2 \right] (\nabla \bar{V} + (\nabla \bar{V})^T)$

The stress components are given by:

$\bar{\tau}_{\bar{x}\bar{x}} = \bar{\tau}_{\bar{y}\bar{y}} = 0$ and $\bar{\tau}_{\bar{x}\bar{y}} = \bar{\tau}_{\bar{y}\bar{x}} = \mu(T) \left[\left(\frac{\partial \bar{u}}{\partial \bar{y}} \right) + \left(\frac{n-1}{2} \right) Y^2 \left(\frac{\partial \bar{u}}{\partial \bar{y}} \right)^3 \right]$ (7)

We rewrite the system of a non-linear partial differential (1) - (4) as follows:

$\frac{\partial \bar{u}}{\partial \bar{x}} + \frac{\partial \bar{v}}{\partial \bar{y}} = 0$ (8)

$\frac{\partial \bar{\tau}_{\bar{x}\bar{x}}}{\partial \bar{x}} + \frac{\partial \bar{\tau}_{\bar{x}\bar{y}}}{\partial \bar{y}} - \frac{\mu(T)}{k} \bar{u} - \rho \frac{\partial \bar{u}}{\partial \bar{t}} = \frac{\partial \bar{p}}{\partial \bar{x}} - \rho g \beta_1 (T - T_{-l}) - \rho g \beta_2 (C - C_{-l}) + \rho g \sin(\varphi)$ (9)

$\frac{\partial \bar{p}}{\partial \bar{y}} = 0$ (10)

$D_c \frac{\partial^2 C}{\partial \bar{y}^2} - \frac{\partial C}{\partial \bar{t}} - K_r^* (C - C_{-l}) = -\frac{D_c T_d}{T_m} \frac{\partial^2 T}{\partial \bar{y}^2}$ (11)

$K \frac{\partial^2 T}{\partial \bar{y}^2} - \rho c_p \frac{\partial T}{\partial \bar{t}} + (4\alpha^2 + h_g)(T - T_{-l}) = 0$ (12)

Method of Solution

The governing equations for non-dimensional conditions are:

$\left. \begin{aligned} x = \frac{\bar{x}}{l}, y = \frac{\bar{y}}{l}, u = \frac{\bar{u}}{V}, \theta = \frac{T - T_{-l}}{T_l - T_{-l}}, p = \frac{\bar{p}l}{\mu_0}, Pe = \frac{\rho l V c_p}{K}, Da = \frac{k}{l^2} \\ , t = \frac{\bar{t}V}{h}, \tau_{xy} = \frac{l}{\mu V} \bar{\tau}_{\bar{x}\bar{y}}, \dot{\gamma} = \frac{l}{V} \dot{\bar{Y}}, \Omega = \frac{C - C_{-l}}{C_l - C_{-l}}, G_{c2} = \frac{\beta_2 l^2 (C_l - C_{-l})}{\mu_0}, \\ Re = \frac{\rho l V}{\mu_0}, \mu(\theta) = \frac{\mu(T)}{\mu_0}, G_{r1} = \frac{\beta_1 l^2 (T_l - T_{-l})}{\mu_0}, S_r = \frac{D_c T_d (T_l - T_{-l})}{V T_m l (C_l - C_{-l})}, \\ W = \frac{\Gamma V}{h}, Sc = \frac{lV}{D_c}, K_r = \frac{lK_r^*}{V}, H_g = \frac{h_g l^2}{K}, \mathcal{K} = \frac{4\alpha^2 l^2}{K}, Fr = \frac{V^2}{gl} \end{aligned} \right\}$ (13)

where V is mean flow velocity, Da is Darcy number, Re is Reynolds number, Pe is Peclet number, \mathcal{K} is radiation parameter. Sc is Schmidt number, S_r is Soret number, H_g is heat generation, T_m is mean temperature, G_{r1} is thermal Grashof number with tilt up, G_{c2} is solutal Grashof number with tilt up, K_r is chemical reaction, W is Weissenberg number, and Fr is Froude number.

By substituting (13) into (8)-(12), we have the following system of the non-dimensional partial differential equations with independent variables y and t and dependent variables u , θ , and Ω .

$\mu(\theta) \left[1 + \frac{3(n-1)}{2} W^2 \left(\frac{\partial u}{\partial y} \right)^2 \right] \frac{\partial^2 u}{\partial y^2} - Re \frac{\partial u}{\partial t} - \frac{\mu(\theta)}{Da} u = \frac{dp}{dx} - G_{r1} \theta - G_{c2} \Omega - \frac{Re \sin(\varphi)}{Fr}$ (14)

$\frac{1}{Sc} \frac{\partial^2 \Omega}{\partial y^2} - \frac{\partial \Omega}{\partial t} - K_r \Omega = -S_r \frac{\partial^2 \theta}{\partial y^2}$ (15)

$\frac{\partial^2 \theta}{\partial y^2} - Pe \frac{\partial \theta}{\partial t} + (H_g + \mathcal{K}) \theta = 0$ (16)

With boundary conditions (after substituting the equations (13) into equations (5) and (6)), we have:

$$u(-1) = u(1) = 0 \quad (17)$$

$$\Omega(-1) = 0, \Omega(1) = 1 \quad (18)$$

$$\theta(-1) = 0, \theta(1) = 1 \quad (19)$$

Solution of the heat and the concentration equations

Using the separating variables method to solve the heat equation (16) with boundary conditions (19) and the concentration equation (15) with boundary conditions (18), assuming that $\theta(y, t) = e^{i\omega t} \theta_0(y)$ and $\Omega(y, t) = e^{i\omega t} \Omega_0(y)$, respectively, where ω is the frequency of oscillation, we obtain the solution of the heat equation and the concentration equation, which are:

$$\theta_0(y) = \left(\frac{e^{3\sqrt{\mathcal{A}}}}{-1+e^{4\sqrt{\mathcal{A}}}} \right) e^{y\sqrt{\mathcal{A}}} + \left(\frac{e^{\sqrt{\mathcal{A}}}}{-1+e^{4\sqrt{\mathcal{A}}}} \right) e^{-y\sqrt{\mathcal{A}}}, \quad \Omega_0(y) = \frac{(\mathcal{A}+\mathcal{B}-S_r S_c)}{(\mathcal{A}+\mathcal{B})(e^{4\sqrt{\mathcal{B}}}-1)} \left(e^{(3+y)\sqrt{\mathcal{B}}} - e^{(1-y)\sqrt{\mathcal{B}}} \right) - \frac{S_r S_c \csc[2\sqrt{\mathcal{A}}] \sin[(1+y)\sqrt{\mathcal{A}}]}{\mathcal{A}+\mathcal{B}}$$

where $\mathcal{A} = i\omega Pe - H_g - \mathcal{K}$, $\mathcal{B} = S_c(K_r + i\omega)$.

Solution of motion equations

To solve the momentum equation for oscillatory flow, we defined Reynold's variation for the viscosity model with temperatures as $\mu(\theta) = e^{-\varepsilon\theta}$, see [8]; Let

$$u(y, t) = \mathcal{U}(y)e^{i\omega t}, \quad \frac{dp}{dx} = -\lambda e^{i\omega t} \quad (20)$$

By using the Maclaurin series, we get:

$$\mu(\theta) = 1 - \varepsilon\theta, \quad \varepsilon \ll 1 \quad (21)$$

where ω is the frequency of oscillation and λ is a real constant. The viscosity is fixed at $\varepsilon = 0$.

By substituting equations (20) and (21) into the momentum equation (14), we get:

$$(1 - \varepsilon\theta) \left[1 + \frac{3(n-1)}{2} W^2 e^{2i\omega t} \left(\frac{\partial \mathcal{U}}{\partial y} \right)^2 \right] \frac{\partial^2 \mathcal{U}}{\partial y^2} - \left(i\omega Re + \frac{(1-\varepsilon\theta)}{Da} \right) \mathcal{U} = - \left(\lambda + G_{r1} \theta_0 + G_{c2} \Omega_0 + \frac{Re \sin(\varphi)}{e^{i\omega t} Fr} \right) \quad (22)$$

It is difficult to solve the nonlinear differential equation (22) and thus we propose a perturbation technique method [16] to solve this equation by taking a small value for W . Accordingly, we write:

$$\mathcal{U} = \mathcal{U}_0 + W^2 \mathcal{U}_1 + O(W^4) \quad (23)$$

By substituting equation (23) into equation (22), with boundary conditions $\mathcal{U}(-1) = \mathcal{U}(1) = 0$, then equating the like powers of W , we obtain:

1 - Zeros-order system

$$(1 - \varepsilon\theta) \frac{\partial^2 \mathcal{U}_0}{\partial y^2} - \left(i\omega Re + \frac{(1-\varepsilon\theta)}{Da} \right) \mathcal{U}_0 = - \left(\lambda + G_{r1} \theta_0 + G_{c2} \Omega_0 + \frac{Re \sin(\varphi)}{e^{i\omega t} Fr} \right) \quad (24)$$

with boundary conditions $\mathcal{U}_0(-1) = \mathcal{U}_0(1) = 0$.

2 - First-order system

$$(1 - \varepsilon\theta) \frac{\partial^2 \mathcal{U}_1}{\partial y^2} - \left(i\omega Re + \frac{(1-\varepsilon\theta)}{Da} \right) \mathcal{U}_1 = -(1 - \varepsilon\theta) \frac{3(n-1)}{2} e^{2i\omega t} \left(\frac{\partial \mathcal{U}_0}{\partial y} \right)^2 \frac{\partial^2 \mathcal{U}_0}{\partial y^2} \quad (25)$$

with boundary conditions $\mathcal{U}_1(-1) = \mathcal{U}_1(1) = 0$.

We note that it is difficult to solve equations (24) and (25), and therefore we use the perturbations method again with respect to the parameter ε by considering that it is small. So that let:

$$\mathcal{U}_i = \mathcal{U}_{i0} + \varepsilon \mathcal{U}_{i1} + O(\varepsilon^2), \text{ for } i = 0, 1 \quad (26)$$

And by equating the coefficient of a like power in ε , then the following set of equations are obtained:

(A) Approximation Solution for \mathcal{U}_0

By substituting (26) into (24), we get:

$$(1 - \varepsilon\theta) \frac{\partial^2 (\mathcal{U}_{00} + \varepsilon \mathcal{U}_{01})}{\partial y^2} - \left(i\omega Re + \frac{(1-\varepsilon\theta)}{Da} \right) (\mathcal{U}_{00} + \varepsilon \mathcal{U}_{01}) = - \left(\lambda + G_{r1} \theta_0 + G_{c2} \Omega_0 + \frac{Re \sin(\varphi)}{e^{i\omega t} Fr} \right)$$

By equating the coefficient of like powers in ε , we obtain:

i- Zeros-Order System (ε^0)

$$\frac{\partial^2 \mathcal{U}_{00}}{\partial y^2} - \left(i\omega Re + \frac{1}{Da} \right) \mathcal{U}_{00} = - \left(\lambda + G_{r1} \theta_0 + G_{c2} \Omega_0 + \frac{Re \sin(\varphi)}{e^{i\omega t} Fr} \right)$$

ii- First-Order System (ε^1)

$$\frac{\partial^2 \mathcal{U}_{01}}{\partial y^2} - \left(i\omega Re + \frac{1}{Da} \right) \mathcal{U}_{01} = \theta \left(\frac{\partial^2 \mathcal{U}_{00}}{\partial y^2} - \frac{1}{Da} \mathcal{U}_{00} \right)$$

(B) Approximation Solution for \mathcal{U}_1

By substituting (26) into (25), we get:

$$(1 - \varepsilon\theta) \frac{\partial^2(\mathcal{U}_{10} + \varepsilon\mathcal{U}_{11})}{\partial y^2} - \left(i\omega Re + \frac{(1-\varepsilon\theta)}{Da}\right) (\mathcal{U}_{10} + \varepsilon\mathcal{U}_{11}) = -(1 - \varepsilon\theta) \frac{3(n-1)}{2} e^{2i\omega t} \left(\frac{\partial \mathcal{U}_0}{\partial y}\right)^2 \frac{\partial^2 \mathcal{U}_0}{\partial y^2}$$

By equating the coefficient of like powers in ε , we obtain:

i- Zeros-Order System (ε^0)

$$\frac{\partial^2 \mathcal{U}_{10}}{\partial y^2} - \left(i\omega Re + \frac{1}{Da}\right) \mathcal{U}_{10} = -\frac{3(n-1)}{2} e^{2i\omega t} \left(\frac{\partial \mathcal{U}_0}{\partial y}\right)^2 \frac{\partial^2 \mathcal{U}_0}{\partial y^2}$$

ii- First-Order System (ε^1)

$$\frac{\partial^2 \mathcal{U}_{11}}{\partial y^2} - \left(i\omega Re + \frac{1}{Da}\right) \mathcal{U}_{11} = \theta \left(\frac{\partial^2 \mathcal{U}_{10}}{\partial y^2} - \frac{1}{Da} \mathcal{U}_{10} + \frac{3(n-1)}{2} e^{2i\omega t} \left(\frac{\partial \mathcal{U}_0}{\partial y}\right)^2 \frac{\partial^2 \mathcal{U}_0}{\partial y^2}\right)$$

Hence, the fluid velocity is given as:

$$u(y, t) = ((\mathcal{U}_{00} + \varepsilon\mathcal{U}_{01}) + W^2(\mathcal{U}_{10} + \varepsilon\mathcal{U}_{11}))e^{i\omega t} \quad (27)$$

Results and Discussion

We discussed the effects of temperature and concentration on the unsteady oscillation flow of an incompressible Carreau fluid with variable viscosity through an inclined porous channel. Analytical solutions are acquired for the problem by the perturbation technique up to the second-order using MATHEMATICA program. We discussed graphically all solutions obtained under variations of different relevant parameters. The results obtained are graphically presented through Figures (2-16).

Figures-(2-10) illustrate the effects of the parameters K_r , S_c , σ , Da , t , S_r , W , λ , ε , G_{r1} , \mathcal{K} , ω , φ , Fr , Pe , H_g , Re and G_{c2} , respectively, on the velocity. It is found that the velocity profile u achieves its maximum height in the center of the channel (at $y=0$). The speed of the fluid begins to increase and tends to be fixed in the walls $\mp l$, particularly at the boundary conditions. Figure-2 illustrates the influence of the parameters K_r and S_c on the velocity distribution function u vs. y . It is found that the velocity profile u decreases with increasing K_r and S_c , respectively. Figure-3 shows that the velocity profile u rises with increasing Da , while u decreases with increasing σ when $-1 < y < 0.2$ and u increases with increasing σ when $0.2 < y < 1$. We noted that the velocity profile u decreases with increasing t while u rises with increasing S_r , as shown in Figure-4. Figure-5 illustrates the influences of the parameters W and λ on the velocity distribution function u vs. y . It is found that the velocity profile u rises with increasing λ , while u decreases with increasing W when $-1 < y < 0$ and u increases with increasing W when $0 < y < 1$. Figure-6 contains the velocity profile behaviour under different ε and G_{r1} values. It is indicated that the velocity profile rises with increasing ε and G_{r1} when $0.5 < y < 1$ and u decreases with increasing ε and G_{r1} when $-1 < y < 0.5$. Figure-7 demonstrates that the velocity profile u decreases by increasing ω , while u increases with increasing \mathcal{K} when $-1 < y < 0.15$ and u decreases with increasing \mathcal{K} when $0.15 < y < 1$. We noted that the velocity profile u increases with increasing φ and u decreases with increasing Fr , as shown in Figure-8. Figures- 9 and 10 show that the velocity profile u rises with increasing the parameters Pe , H_g , Re and G_{c2} , respectively.

Figures- (11-12) illustrate the effects of the parameters Pe , H_g , ω and \mathcal{K} , respectively, on the temperature function θ . It is found that the temperature of fluid θ rises with increasing H_g , while it decreases with increasing Pe , as shown in Figure-11. Figure-12 demonstrates that the temperature of fluid θ is reduced by increasing ω and rises with increasing \mathcal{K} . Figures- (13-16) illustrate the effects of the parameters K_r , S_c , t , S_r , Pe , H_g , ω and \mathcal{K} , respectively, on the concentration function Ω . Figures- 13 and 14 indicate that the fluid concentration Ω decreases by increasing the parameters K_r , S_c , t and S_r , respectively. In Figure-15, we notice that the concentration Ω increases with the increase in Pe and decreases with the increase in H_g . The last Figure-16 shows that the concentration Ω increases with the increase in ω and decreases with the increase in \mathcal{K} .

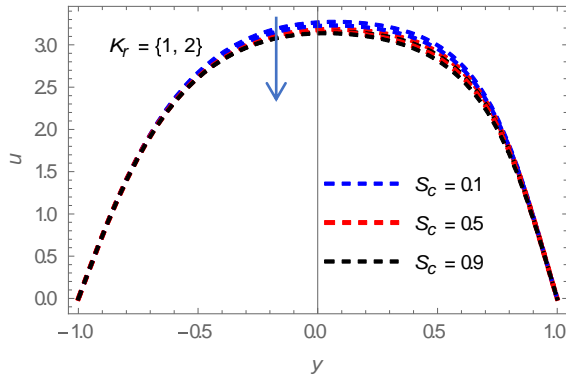


Figure 2-Velocity profile for K_r and S_c with $n = 3, \varepsilon = 0.1, t = 0.1, W = 0.1, \omega = 1, S_r = 0.5, G_{r1} = 1, G_{c2} = 1, Re = 0.5, Pe = 1, \mathcal{K} = 1, H_g = 1, Da = 0.8, \lambda = 1.5, Fr = 0.1, \sigma = \pi/4, \varphi = \pi/6$.

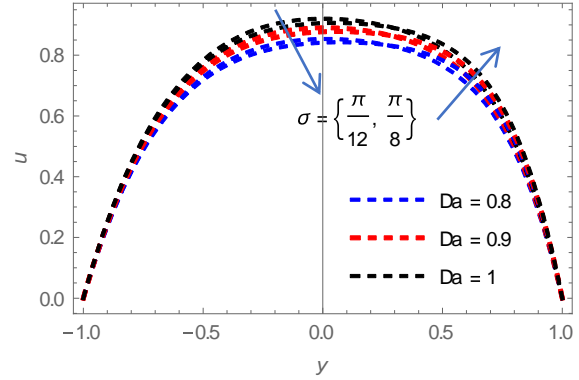


Figure 3-Velocity profile for σ and Da with $n = 3, \varepsilon = 0.1, t = 0.1, W = 0.1, \omega = 1, K_r = 2, S_c = 0.6, S_r = 0.5, G_{r1} = 1, G_{c2} = 1, Pe = 1, Re = 0.5, \mathcal{K} = 1, H_g = 1, \lambda = 1.5, Fr = 0.1, \varphi = \pi/6$.

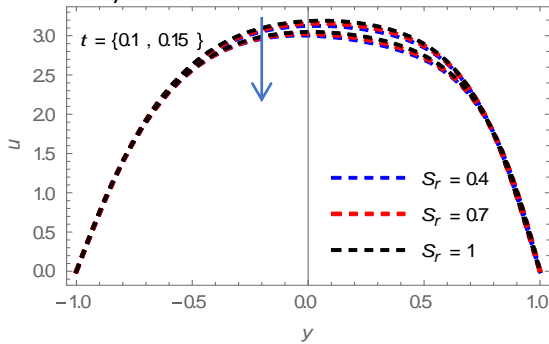


Figure 4-Velocity profile for t and S_r with $n = 3, \varepsilon = 0.1, W = 0.1, \omega = 1, K_r = 2, S_c = 0.6, G_{r1} = 1, G_{c2} = 1, Re = 0.5, Pe = 1, \mathcal{K} = 1, H_g = 1, Da = 0.8, \lambda = 1.5, Fr = 0.1, \sigma = \pi/4, \varphi = \pi/4$.

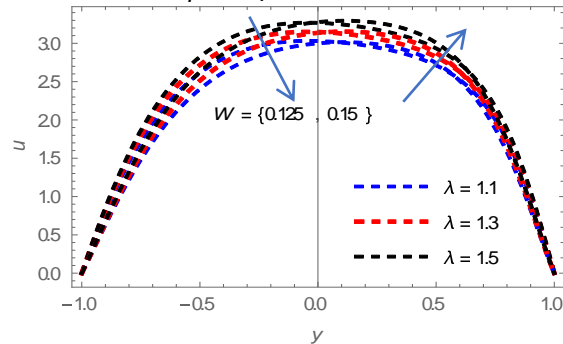


Figure 5- Velocity profile for W and λ with $n = 3, \varepsilon = 0.1, t = 0.1, G_{c2} = 0.1, \omega = 1, K_r = 2, S_c = 0.6, S_r = 0.5, G_{r1} = 1, Re = 0.5, Pe = 1, \mathcal{K} = 1, H_g = 1, Da = 0.8, Fr = 0.1, \sigma = \pi/4, \varphi = \pi/4$.

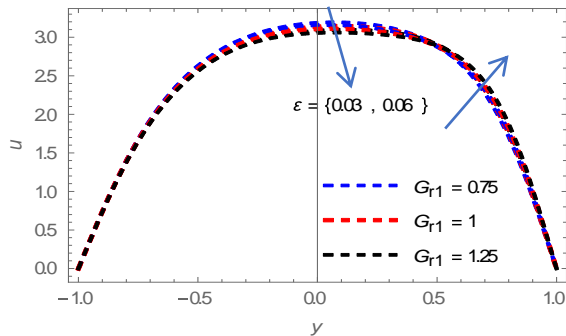


Figure 6- Velocity profile for ε and G_{r1} with $n = 3, t = 0.1, W = 0.1, \omega = 1, K_r = 2, S_c = 0.6, S_r = 0.5, G_{c2} = 1, Re = 0.5, Pe = 1, \mathcal{K} = 1, H_g = 1, Da = 0.8, \lambda = 1.5, Fr = 0.1, \sigma = \pi/4, \varphi = \pi/4$.

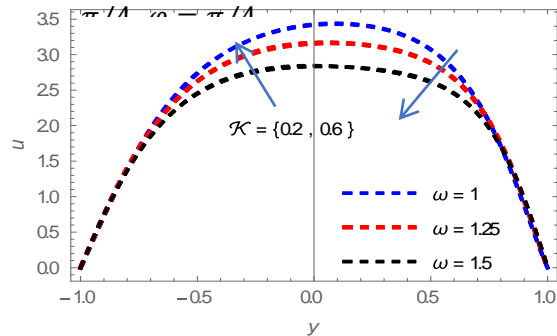


Figure 7- Velocity profile for \mathcal{K} and ω with $n = 3, \varepsilon = 0.1, t = 0.1, W = 0.1, K_r = 2, S_c = 0.6, S_r = 0.5, G_{r1} = 1, G_{c2} = 1, Re = 0.5, Pe = 1, H_g = 1, Da = 0.8, \lambda = 1.5, Fr = 0.1, \sigma = \pi/4, \varphi = \pi/4$.

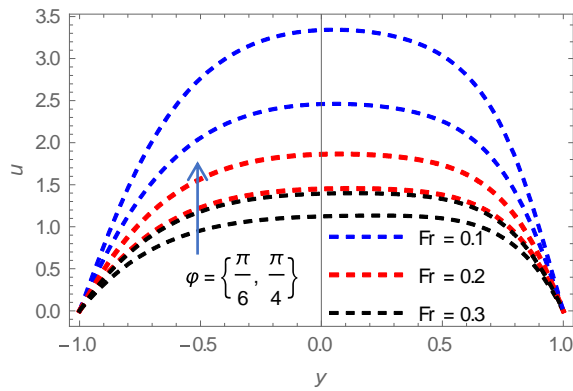


Figure 8- Velocity profile for φ and Fr with $n = 3, t = 0.1, W = 0.1, \varepsilon = 0.1, \omega = 1, K_r = 2, S_c = 0.6, S_r = 0.5, G_{r1} = 1, G_{c2} = 1, Re = 0.5, Pe = 1, \mathcal{K} = 1, H_g = 1, Da = 0.8, \lambda = 1.5, Fr = 0.1, \sigma = \pi/4, \varphi = \pi/4$

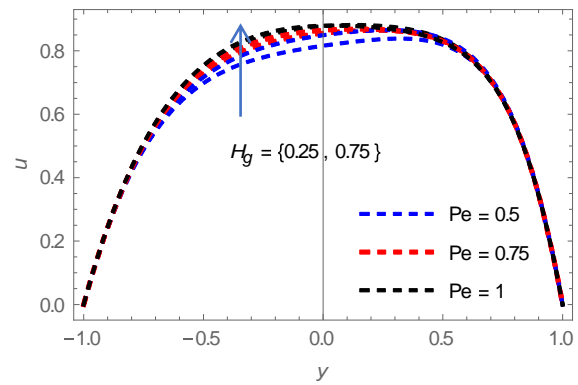


Figure 9- Velocity profile for Pe and H_g with $n = 3, t = 0.1, W = 0.1, \varepsilon = 0.1, \omega = 1, K_r = 2, S_c = 0.6, S_r = 0.5, G_{r1} = 1, G_{c2} = 1, Re = 0.5, \mathcal{K} = 1, Da = 0.8, \lambda = 1.5, Fr = 0.1, \sigma = \pi/4, \varphi = \pi/4$

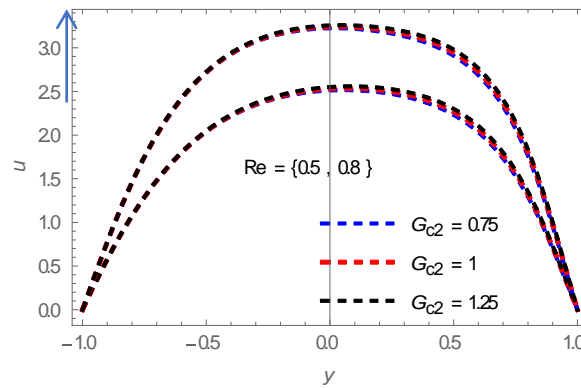


Figure 10- Velocity profile for Re and G_{c2} with $n = 3, \varepsilon = 0.1, t = 0.1, W = 0.1, \omega = 1, K_r = 2, S_c = 0.6, S_r = 0.5, G_{r1} = 1, Pe = 1, \mathcal{K} = 1, H_g = 1, Da = 0.8, \lambda = 1.5, Fr = 0.1, \sigma = \pi/4, \varphi = \pi/4$

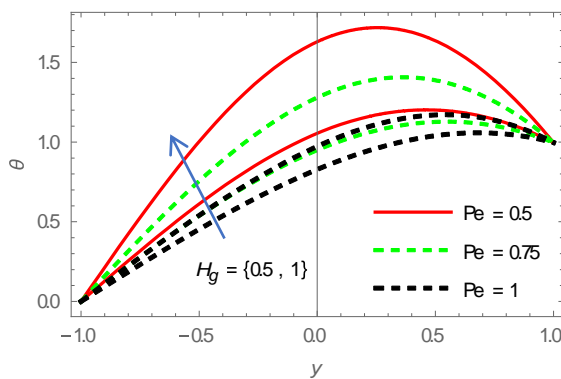


Figure 11- Temperature distributions for H_g and Pe with $t = 0.1, \omega = 0.75, \mathcal{K} = 0.75$.

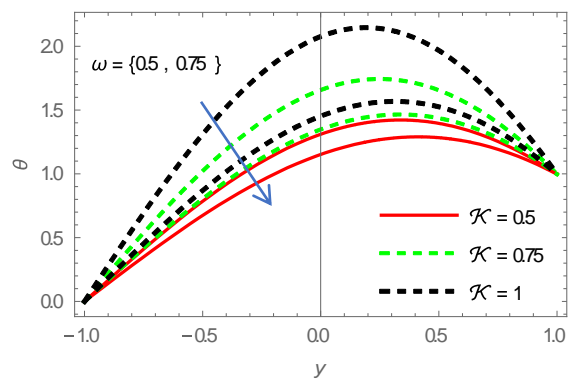


Figure 12- Temperature distributions for \mathcal{K} and ω with $t = 0.1, Pe = 0.75, H_g = 0.75$.

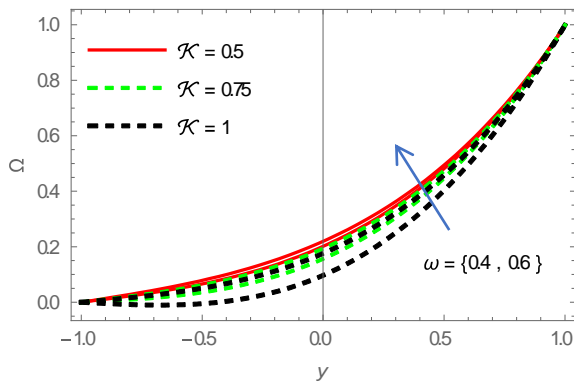


Figure 13- Concentration distributions for \mathcal{K} and ω with $t = 0.1, K_r = 2, S_c = 0.5, S_r = 0.3, Pe = 0.75, H_g = 1$.

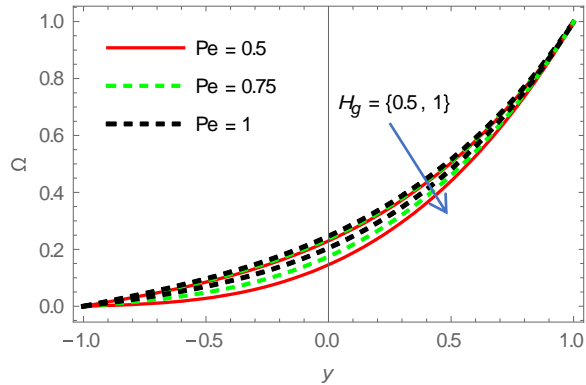


Figure 14- Concentration distributions for H_g and Pe with $t = 0.1, K_r = 2, S_c = 0.5, S_r = 0.3, \omega = 0.5, \mathcal{K} = 0.75$.

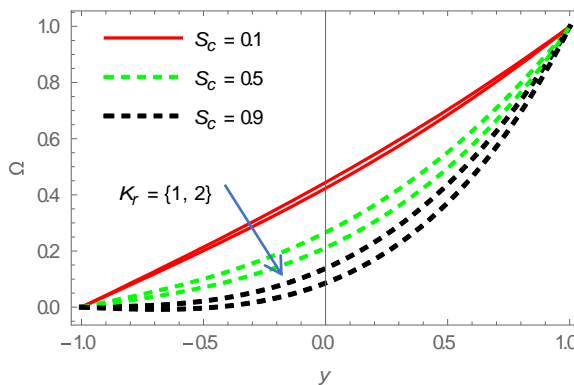


Figure 15- Concentration distributions for S_c and K_r with $t = 0.1, Pe = 0.75, S_r = 0.3, \omega = 0.5, \mathcal{K} = 0.75, H_g = 1$.

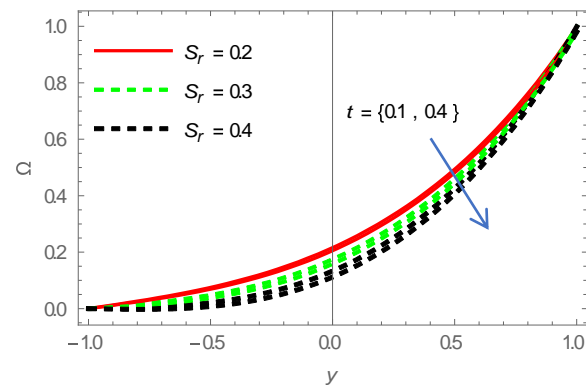


Figure 16- Concentration distributions for S_r and t with $K_r = 2, Pe = 0.75, S_c = 0.5, \omega = 0.5, \mathcal{K} = 0.75, H_g = 1$.

Concluding Remarks

We refer in this section to the most important parameters that affected the unsteady oscillation flow of an incompressible Carreau fluid through an inclined porous channel. We found the velocity function by using the perturbation technique and MATHEMATICA-12 program. We discussed graphically all solutions obtained under variations of different relevant parameters. The main findings can be summarized as follows:

- The velocity flow rises with the increase of $Da, S_r, \lambda, \varphi, Pe, H_g, Re$ and G_{c2} , while decreases with the increase of K_r, S_c, t, ω and Fr .
- The velocity is decreasing function vs. ε, G_{r1} and W , respectively, when $-1 < y < 0$, while it is an increasing function when $0 < y < 1$.
- The velocity flow rises with the increase of \mathcal{K} when $-1 < y < 0.15$, while it decreases when $0.15 < y < 1$.
- The temperature of fluid rises with increasing \mathcal{K} and H_g , while it decreases with increasing ω and Pe .
- The concentration of fluid rises with increasing ω and Pe , while it decreases with increasing $\mathcal{K}, H_g, K_r, S_c, t$ and S_r .
- Over time, the fluid's temperature and concentration decrease, which affects the movement of the viscous Carreau fluid, according to its location in the flow channel, where the fluid is increasingly flowing near the upper wall of the channel while the movement of the fluid decreases near the lower wall.

References

1. Soundalgekar V.M. and Bhat J.P. **1971**. Oscillatory channel flow and heat transfer. *Int J Pure and App Math* (15): 819-828.
2. Raptis A.A. and Perdikis C.P. **1985**. Oscillatory flow through a porous medium by the presence of free convective flow. *International Journal of Engineering Science*, **23**(1): 51-55.
3. Tabakova S., Nikolova E. and Rade St. **2014**. Carreau model for oscillatory blood flow in a tube, Application of Mathematics in Technical and Natural Sciences, *AIP Publishing*, (1629): 336-343. <https://doi.org/10.1063/1.4902290>.
4. Khudair W.S. and Al-Khafajy D.G.S. **2018**. Influence of Heat Transfer on MHD Oscillatory Flow for Williamson Fluid with Variable Viscosity Through a Porous Medium, *International Journal of Fluid Mechanics & Thermal Sciences*, Science Publishing Group, **4**(1): 11-17.
5. Sasikumar J., Harinisha N. and Anitha S. **2019**. MHD oscillatory flow through porous medium in rotating wavy channel with heat source, *AIP Conference Proceedings* (2112): 020104 , <https://doi.org/10.1063/1.5112289>.
6. Sharp K.M., Carare R.O. and Martin B.A. **2019**. Dispersion in porous media in oscillatory flow between flat plates: applications to intrathecal, periarterial and paraarterial solute transport in the central nervous system. *Fluids Barriers CNS* **16**, 13. <https://doi.org/10.1186/s12987-019-0132-y>.
7. Person J.R.A. **1977**. Variable-viscosity flows in channels with high heat generation, *J. Fluid Mech.*, **83**(1): 191-206.
8. Al-Khafajy D.G.S. **2016**. Effects of heat-transfer on MHD oscillatory flow of Jeffrey fluid with variable viscosity through porous medium. *Advances in Applied Science Research*, **7**(3): 179-186.
9. Tanveer A., Hayat T. and Alsaedi A. **2018**. Variable viscosity in peristalsis of Sisko fluid, *Appl. Math. Mech.*, Springer, **39**(4): 501–512. <https://doi.org/10.1007/s10483-018-2313-8>.
10. Pattnaik J.R., Dash G.C. and Singh S. **2017**. Diffusion-thermo effect with hall current on unsteady hydromagnetic flow past an infinite vertical porous plate, *Alexandria Engineering Journal*, **65**(1): 13-25.
11. Hussain A., Akbar S., Sarwar L., Nadeem S. and Iqbal Z. **2019**. Effect of time dependent viscosity and radiation efficacy on a non-Newtonian fluid flow. *Heliyon-ELSEVIER*, **5**, 1-32. doi: 10.1016/j.heliyon.2019. e01203.
12. Hasona W.M., Almalki N.H., ElShekhipy A.A. and Ibrahim M.G. **2019**. Thermal radiation and variable electrical conductivity effects on MHD peristaltic motion of Carreau nanofluids: Radiotherapy and thermo-therapy of oncology treatment. *Heat Transfer-Asian Res.*, 1-19. <https://doi.org/10.1002/htj.21415>.
13. Al-Khafajy D.G.S. **2020**. Radiation and Mass Transfer Effects on MHD Oscillatory Flow for Carreau Fluid through an Inclined Porous Channel, *Iraqi Journal of Science*, **61**(6): 1425-1432.
14. Haroun H. **2007**. Non-linear peristaltic flow of a fourth grade fluid in an inclined asymmetric channel, *Computational Materials Science*, **39**(2): 324-333.
15. Lu D.C., Farooq U., Hayat T., Rashidi M.M. and Ramzan M. **2018**. Computational analysis of three layer fluid model including a nanomaterial layer, *International Journal of Heat and Mass Transfer* (122): 222–228.
16. Nayfeh A.H. **1981**. *Introduction to Perturbation Techniques*, Wiley, New York.